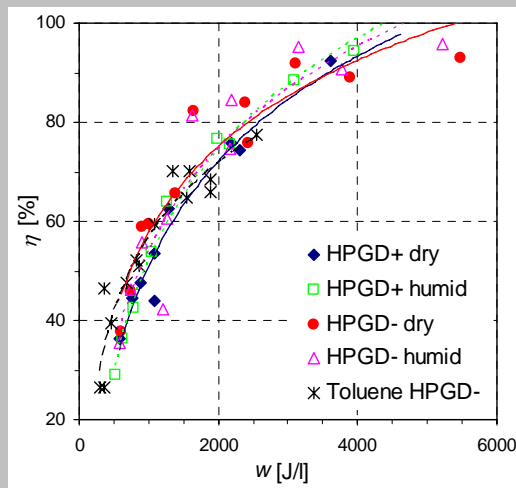


**Summary:** In this article, a direct-current (DC) discharge in atmospheric pressure air as a source for pollution control is presented. The investigated continuous discharge occurring between two metal electrodes is of the glow type. The discharge generated a highly ionized, non-equilibrium air plasma with gas temperatures of 1 500–2 500 K. Single and multiple discharges of this type were successfully tested in glass and copper tube reactors for the abatement of selected VOCs (cyclohexanone and toluene). Depending on the reactor type, discharge parameters and the energy density, abatement efficiencies of 30–95 % were obtained, with energy costs of 200–1 000 eV/molecule. The thermal VOC decomposition in the discharge was coupled with radical-induced volume reactions. It was found that extending the radical-dominated decomposition phase yielded a better performance. The VOCs tested were converted to some gaseous and some condensed products. Copper electrode surfaces influenced the character of the condensed products and seemed to have a certain catalytic effects on the process.



Removal efficiency,  $\eta$ , as a function of the energy density  $w$ . Both polarities of HPGD in dry and humid air, 5-point glass tube reactor, cyclohexanone 2 000 ppm. Toluene 2 000 ppm in negative HPGD has been added for comparison.

## DC Glow Discharge in Atmospheric Air as a Source for Volatile Organic Compounds Abatement

Zdenko Machala<sup>\*1</sup>, Emmanuel Marode,<sup>2</sup> Marcela Morvová,<sup>1</sup> Peter Lukáč<sup>3</sup>

<sup>1</sup> Department of Astronomy, Earth Physics and Meteorology, Faculty of Mathematics, Physics and Informatics, Comenius University, Mlynská dolina F2, 84248 Bratislava, Slovakia, tel. +421-2-60295676, fax: +421-2-65425882, E-mail: machala@fmph.uniba.sk

<sup>2</sup> Laboratoire de Physique des Gaz et des Plasmas, Université Paris XI, Supélec, Plateau de Moulon, 91192 Gif sur Yvette, France

<sup>3</sup> Department of Experimental Physics, Faculty of Mathematics, Physics and Informatics, Comenius University, Mlynská dolina F2, 84248 Bratislava, Slovakia

Received: December 1, 2004; Revised January 14, 2005; Accepted January 20, 2005; DOI: 10.1002/ppap.200400084

**Keywords:** DC Discharges, non-thermal plasma, pollution control, volatile organic compounds

### Introduction

Atmospheric pressure non-equilibrium air plasmas are of considerable interest for a wide range of applications such as air pollution control, bio-decontamination, plasma-assisted combustion, material processing, surface treatment, and electromagnetic wave shielding. Desirable conditions are high electron densities (above  $10^{12}$  cm<sup>-3</sup>) and relatively low gas temperatures (below 2 000 K).

Various types of atmospheric pressure DC or AC glow discharges as sources of nonequilibrium plasmas have received renewed attention during the past few years, for example micro-hollow cathode discharges<sup>[1]</sup>, discharges with one or both electrodes covered by water<sup>[2-3]</sup>, AC

pseudoglow discharges<sup>[4-5]</sup>, low current DC glow discharges<sup>[6]</sup>, and simple DC glows between two metal electrodes<sup>[7-13]</sup>. The subject of our research was a DC glow discharge in atmospheric pressure air as a source for volatile organic compound (VOC) abatement. This discharge, previously also known as high pressure glow discharge (HPGD),<sup>[10-11]</sup> does not use dielectric barrier layers, and as such should not be identified with the recently widely investigated atmospheric pressure glow discharges (APGD). The DC glow discharge studied here has the advantage of producing relatively large volumes of fairly homogeneous plasma. In addition, DC operation enables easy control of the current and plasma properties, making it attractive for various applications. DC-driven atmospheric air discharges similar with our discharge type

have also been applied for the abatement of toluene and other VOCs.<sup>[14-20]</sup>

In this paper, brief characteristics of a DC glow discharge in ambient atmospheric pressure air are provided, which were obtained by electrical and spectroscopic measurements. This discharge type is then presented at low currents as a source for the abatement of VOCs, following previous studies.<sup>[10-11]</sup> The importance of various parameters on the performance of the VOC abatement process are discussed. Results from the original study performed at the LPGP, University Paris XI, France, have been combined with results obtained at Comenius University, Slovakia.

## Experimental Part

Two DC power supplies were used, placed in series with ballast resistors, to sustain the discharge. These were a Del High Voltage RHVS (60 kV, 5 mA), and Universal Voltronics Mintrol (30 kV, 150 mA). The ballast resistor was used to stabilize the discharge. Its value was chosen experimentally, typically about 500 k $\Omega$ , depending on the operating discharge current. The discharge voltage was measured with a high voltage probe (Tektronix T6015A 1000 x, 3 pF, 100 M $\Omega$ ). The discharge current recorded across a 50  $\Omega$  resistor and the discharge voltage measured by the probe were processed by digitizing oscilloscopes (400 MHz Tektronix DSA 602 and 500 MHz Tektronix TDS 544 A). The discharge was typically applied in point-to-plane geometry; we used rhodium points opposite to copper planes as electrodes.

Spatially resolved optical emission spectroscopy and electrical diagnostics were employed to characterize the discharge properties. An optical set-up shown in Figure 1 consists of a Jobin Yvon monochromator HR 640 (200-700 nm, resolution 0.1 nm) combined with a photomultiplier tube (Hamamatsu C659S). The PMT signal is processed by a 400 MHz digitizing oscilloscope (Tektronix DSA 602) linked with a PC. For spectroscopic studies, the discharge was operated in a cylindrical chamber

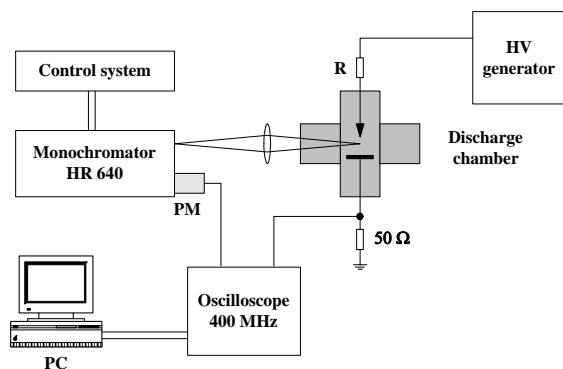


Figure 1. Schematic of the experimental set-up used for the emission spectroscopy of the DC discharge

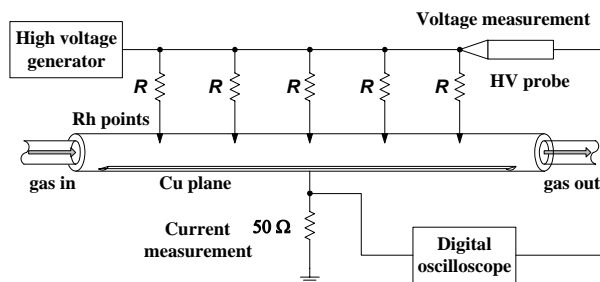


Figure 2. Glass tube reactor with 5 parallel points and its electric circuit.

with about 1 l volume. A digital camera (Nikon Coolpix 990) was used for photo-documentation of discharges.

Several types of discharge reactors were used for the VOC abatement. Most of experiments were performed in a 21 cm long glass tube of 1 cm diameter, with 5 parallel rhodium points and one plane copper electrode, as shown in Figure 2. This reactor allowed operating from 1 to 5 discharges in parallel, with independently variable interelectrode distance. The discharges were supplied from the same high voltage generator but each point was ballasted independently (usually 500 k $\Omega$ ).

A similar discharge reactor consisting of a glass tube with 5 point-to-plane gaps placed in series was developed in order to decrease the energy losses in the ballast resistors of each discharge. We also tested a cylindrical discharge reactor consisting of a 50 cm long copper tube of 25 mm diameter, with a 6 mm thick copper threaded rod central electrode. This reactor enabled longer contact of the treated gas with the catalytic copper surfaces.

Cyclohexanone and toluene were chosen as VOC representatives due to their wide industry use and different properties. Cyclohexanone is a non-aromatic cyclic ketone that, to the best of our knowledge, has been studied for the plasma abatement only in the previous work of this group.<sup>[10-11]</sup> Toluene is an aromatic hydrocarbon that is one of the most typically treated VOCs in plasma abatement processes.

Experiments aimed at VOC abatement were carried out in the flowing dry or humid air. The gas flow system is shown in Figure 3. The air flux was divided into two or three branches controlled by the flowmeters (Sho RATE Brooks) with different ranges. One branch passed through a bubbler with a liquid VOC, thus enriching the air with the VOC vapors at their saturated pressure. Another branch could optionally pass through the bubbler with water, thus providing water vapors at their saturated pressure. The adjustment of the flowmeters allowed setting the VOC and H<sub>2</sub>O concentrations in the gas. Usually, the relative humidity of the humid air was close to 100 % at a given temperature. The three branches rejoined in the mixing chamber and the VOC-enriched air was then lead into the discharge reactor. Gas flow rates of 1-10 slpm (standard liters per minute) were typically used.

Infrared absorption spectroscopy was used as a principal diagnostic method. A Fourier transform infrared spectrometer (FT-IR Bruker IFS 45) was employed,

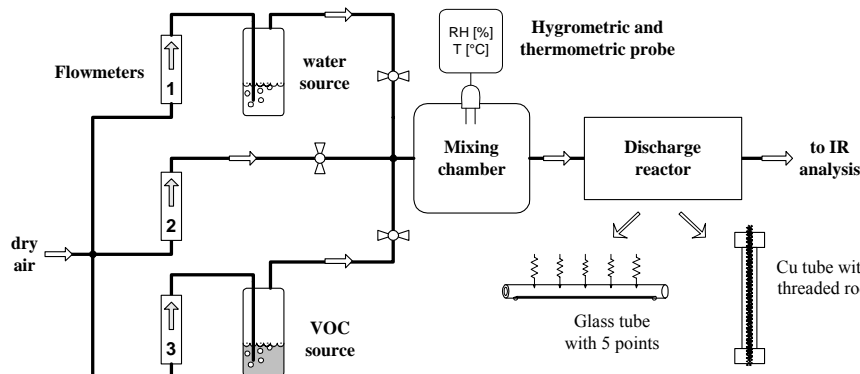


Figure 3. Schematic of the gas flow system.

working in the middle infrared region ( $4\,000\text{--}600\text{ cm}^{-1}$ ) with best resolution of  $0.5\text{ cm}^{-1}$ . A 10 cm long brass gas cell with KBr or  $\text{CaF}_2$  windows was used. Alternatively, a long-path gas cell was used, which had an adjustable optical length between 0.8 and 8 m, with gold mirrors and ZnSe windows. The long path cell allowed detecting very low concentrations of the gaseous by-products. The spectrometer was equipped with the infrared microscope able to work in transmission or reflection regime. This allowed analyzing liquid and solid samples and surfaces, especially deposits formed in the process, and the surfaces of treated electrodes.

The concentrations of VOCs and dominant gaseous products were calculated from the absorbance of their calibrated characteristic bands in the infrared spectra. VOC concentrations from 500 to 6 000 ppm were used, most typically 2 000 ppm. The temperature and the relative humidity were measured in the mixing chamber by a capacitive hygroscopic and thermometric probe (Hanna HI 8564).

## Results and Discussion

### DC Glow Discharge

The DC atmospheric pressure air discharge under study was a stable continuous discharge regime with no pulses. It operated with DC currents from 1.6 to 150 mA, and DC voltages from a few kilovolts to a few hundred volts. The interelectrode distance could be varied from 1 mm to a few cm, depending on the gas flow conditions and the current. The voltage-current characteristic of the discharge in ambient air had a negative slope. In contrast, the discharge power increased with the current. The discharge was ignited by a streamer-to-spark transition, but the ballast resistor immediately limited the spark current. However, the ballast resistor was chosen so that the limiting current was large enough that the discharge, after extinction of the initial spark phase, entered a state of permanent conduction. The ballast-limited current then controlled this pulseless discharge regime. The electrode material was not crucial for the discharge mechanism. Electrodes with a small radius of curvature (pins) permitted easier discharge ignition. A more detailed description of this discharge type

can be found in ref.<sup>[12]</sup> and ref.<sup>[13]</sup> Figure 4 shows a photograph of a typical DC glow discharge in ambient air at atmospheric pressure operating at low flow velocity (about  $0.2\text{ m.s}^{-1}$ ) and a current of 5 mA, with the interelectrode distance of 7 mm.

The spectra emitted by the DC air discharge in the UV-VIS region were recorded for various discharge parameters. The  $\text{N}_2$  ( $\text{C}^3\Pi_u\text{--B}^3\Pi_g$ ) spectral system was then used to measure the rotational and vibrational temperatures,  $T_r$  and  $T_v$ , by comparison with simulated spectra. In atmospheric pressure plasmas, the rotational temperature is close to the gas temperature ( $T_r \approx T_g$ ) owing to fast collisional relaxation. The gas temperature,  $T_g$ , measured at the centerline of the discharge column, varied typically in the range of 1 500–2 500 K. The current, the voltage and the gas flow velocity control the energy density deposited in the discharge, and thus the gas heating. At a given low flow velocity of ambient air through the discharge,  $T_g$  increases and  $T_v$  decreases with increasing current, as shown in Figure 5. The measured vibrational temperatures,  $T_v$ , of the excited states were around 4 000 K.

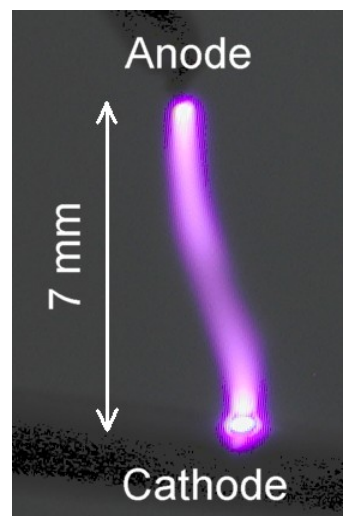


Figure 4. DC glow discharge in ambient atmospheric pressure air,  $I = 5\text{ mA}$ ,  $U = 1.7\text{ kV}$ ,  $d = 7\text{ mm}$ .

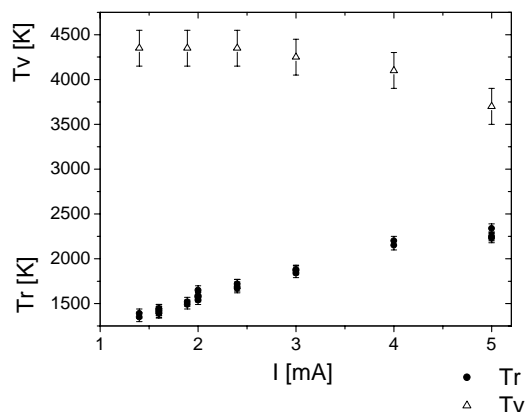


Figure 5. Rotational and vibrational temperatures as functions of the discharge current in ambient air,  $d = 7$  mm.

These temperatures are higher than the gas temperature and therefore suggest that the plasma was in a state of thermal non-equilibrium.

Besides temperature measurements, optical emission spectroscopy diagnostics also provided spatial distributions of the emission intensity. The axial emission intensity profiles indicated the stratification into dark and bright layers, typical of low pressure glow discharges. The positive column occupied most of the interelectrode space, with approximately uniform electric field strength. The voltage drop across the very thin region next to the cathode was close to 370 V, a typical cathode fall of glow discharges in air with Cu cathode.<sup>[21]</sup> The calculated reduced field strengths  $E/N$  were in the range of 40–65 Td.

The radial emission intensity profiles were used to measure the diameter of the positive column. The measured discharge diameter was then used to estimate the plasma volume and the current density. Knowing the field strength, the current density and the gas density (calculated from the measured  $T_g$ ) enabled the plasma conductivity to be estimated, and hence the electron density,  $n_e$ , using Ohm's law.<sup>[8,21]</sup> The measured discharge diameters ranged from 0.4 to 2 mm, depending on the current, the gas flow velocity, and the gas temperature. The corresponding current densities were between 0.1 and 10 A.cm<sup>-2</sup> and the estimated electron densities,  $n_e$ , were in the range of 10<sup>12</sup>–10<sup>13</sup> cm<sup>-3</sup>. The measured current densities were lower than those typical of arcs are. Moreover, the high values of  $n_e$  at gas temperatures between 1 500 and 2 500 K confirmed that the discharge plasma was in thermal non-equilibrium, since the LTE values of  $n_e$  in atmospheric pressure air are about 10<sup>2</sup>, 10<sup>6</sup>, and 10<sup>9</sup> cm<sup>-3</sup>, for the temperatures of 1 500, 2 000, and 2 500 K, respectively.

### VOC Abatement

The studied DC discharge of both polarities was applied for the abatement of selected VOCs (cyclohexanone and toluene) in dry and humid air. The process was characterized by the following fundamental parameters:

- Removal efficiency (or relative removal rate),  $\eta$  [%]
- Energy density (or specific energy input)  $w$  [J.l<sup>-1</sup> or Wh.m<sup>-3</sup> where 1 J.l<sup>-1</sup> = 1/3.6 Wh.m<sup>-3</sup>]
- Energy costs [eV/molecule or kWh.kg<sup>-1</sup>]\*, where 1 eV/molecule = 0.275 (0.293) kWh.kg<sup>-1</sup> for cyclohexanone (toluene)
- Character and concentration of products.

In the glass tube reactor with 5 discharges, the achieved removal efficiencies varied from 30 to 96 % for cyclohexanone and from 13 to 77 % for toluene. The removal efficiency increased with increasing energy density  $w$  for both studied compounds, in both polarities, and in dry as well as humid air, as shown in Figure 6. This increase was not linear – a saturation effect was observed. The experimental points were fitted by logarithmic trend lines, which indicated that the VOC concentration decreased exponentially with increasing  $w$ . This trend is typical for non-thermal plasma VOC treatment. Since the toluene curves were very similar to those of cyclohexanone, only one is shown for clarity.

Energy costs as a function of  $w$  for cyclohexanone treatment are shown in Figure 7. These curves were again very similar to those of toluene, so just one is shown. With both VOCs, energy costs increased approximately exponentially with  $w$ , from 200 to 1 000 eV/molecule (corresponding to an energy efficiency between 3.6 and 18 g.kWh<sup>-1</sup>), which is comparable with the results of other studies.<sup>[19–20,22]</sup> This result suggests that it is more convenient to work at low  $w$  to decrease energy costs, although  $\eta$  is lower. Figure 6 and 7 also show very small differences between the effects of positive or negative discharge polarity and the presence of water vapor. However, humid air and the negative polarity yielded slightly higher efficiency and lower energy costs for the same  $w$ . This is probably in part caused by enhanced formation of highly reactive OH radicals in the humid air, as suggested by many related publications such as ref.<sup>[22–25]</sup>

In the glass tube 5-point reactor and in the studied range of VOC concentrations (500–6 000 ppm), almost no influence of the initial concentration on the removal efficiency was observed for either of the VOCs studied. This is in contrast with the typical trend observed in non-thermal plasma treatment of VOCs, where efficiency decreases with concentration. It is hypothesized that this effect might be caused by the flow conditions coupled with the volume ratio of the chemically active zones (discharge channels and their surroundings) with respect to the zones of low activity (e.g. near reactor walls) in the reactor. At every specific energy density, a certain amount of the gas will pass through the non-active zones and therefore remain untreated, regardless to the VOC concentration in it. Since the efficiency depends on the energy density, this volume ratio of active and non-active zones in the reactor also somehow depends on the energy density. A rigorous explanation of this effect requires further investigations,

\* In some industry-related works, energy efficiency is used rather than energy costs; energy efficiency [g.kWh<sup>-1</sup>] being the inverted value of energy costs [kWh.g<sup>-1</sup>].

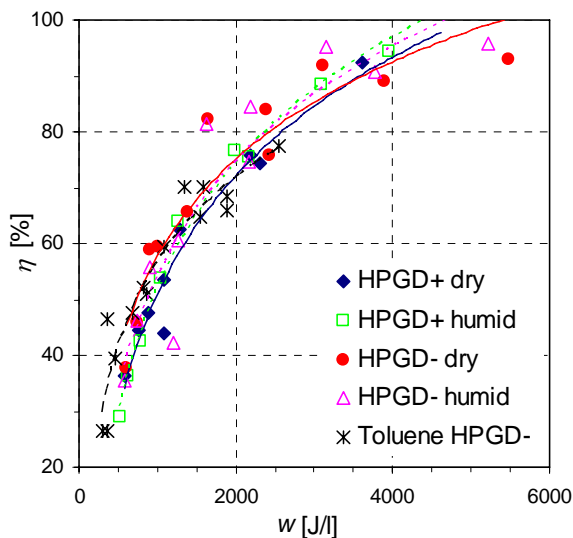


Figure 6. Removal efficiency,  $\eta$ , as a function of the energy density  $w$ . Both polarities of HPGD in dry and humid air, 5-point glass tube reactor, cyclohexanone 2 000 ppm. Toluene 2 000 ppm in negative HPGD has been added for comparison.

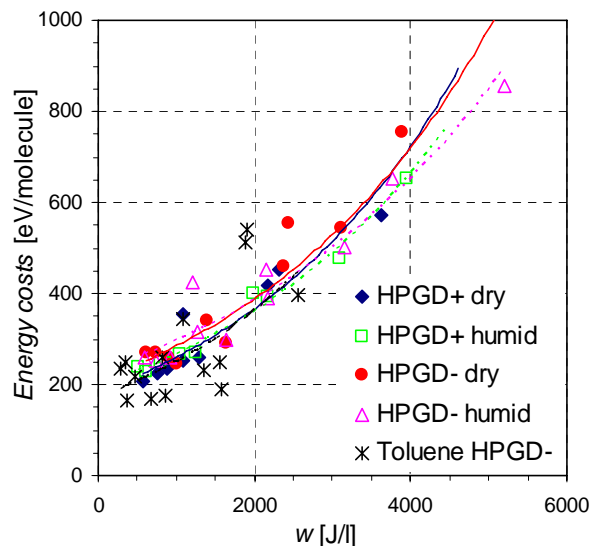


Figure 7. Energy costs as a function of the energy density  $w$ . Both polarities of HPGD in dry and humid air, 5-point glass tube reactor, cyclohexanone 2 000 ppm. Toluene 2 000 ppm in negative HPGD has been added for comparison.

which should also focus at lower VOC concentrations typical of most industrial flue gases. On the other hand, the energy costs decrease with the initial VOC concentration.

As shown previously (Figure 6), the removal efficiency,  $\eta$ , did not increase linearly with the rising energy density,  $w$ . This effect of non-linearity was further studied by comparing the effects of:

- 1 single discharge in the glass tube 5-point reactor,
- 5 parallel discharges in the same reactor,

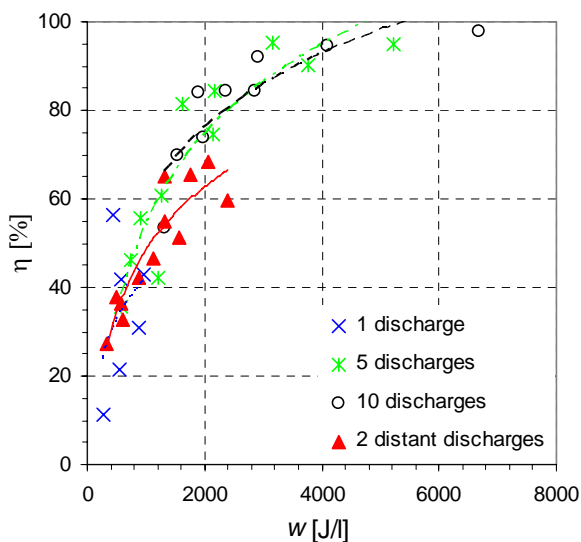


Figure 8. Removal efficiency,  $\eta$ , as a function of the energy density,  $w$ . Glass tube reactors with 1, 5, 10, and 2 distant discharges, negative HPGD, humid air, cyclohexanone 2 000 ppm.

- 10 parallel discharges in two such reactors put in series,
- 2 discharges distant from each other by about 2 m (operated in two 5-point reactors joined in series by a 2 m long hose).

This comparison was performed for both positive and negative HPGD, and for both dry and humid air, with 2 000 ppm cyclohexanone. For better clarity, only the results of the negative polarity in humid air are shown here.

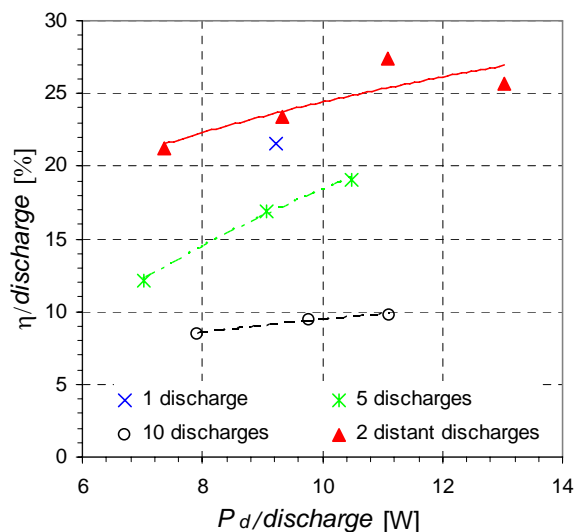


Figure 9. Removal efficiency,  $\eta$ , as a function of the discharge power  $P_d$  at  $Q=1$  slpm, normalized to the number of working discharges. Glass tube reactors with 1, 5, 10, and 2 distant discharges, negative HPGD, humid air, cyclohexanone 2 000 ppm.

The  $\eta$  as a function of  $w$  for 1, 5, 10, and 2 distant discharge systems is shown in Figure 8. A non-linearity (saturation) effect was observed, even with one operated discharge. The total achieved efficiency was higher at the same  $w$  when working with more discharges, except with 10 discharges, which had about the same efficiency as 5 discharges. A certain synergy between the discharges was found, contributing to the total efficiency increase, but this effect had a saturation threshold. In the reactor studied here, this threshold was found with 5 parallel discharges.

The energy density,  $w$ , delivered into the treated bulk gas could be varied by changing either the discharge power,  $P_d$ , or the gas flow rate,  $Q$ , or the number of working discharges. In order to simplify the comparison of the effects of 1, 5, 10 or 2 distant discharges, the gas flow rate was fixed at  $Q = 1$  slpm.  $w$  was then represented by the discharge power  $P_d$ . The  $\eta(P_d)$  curves were normalized by the number of working discharges, i.e.,  $\eta$  and  $P_d$  were divided by the number of discharges. This representation enabled the efficiency of each discharge used to be seen more clearly, as shown in Figure 9. Interestingly, the efficiency per discharge was the highest in the case of 2 distant discharges and the lowest for 10 discharges. The efficiency per discharge for 2 distant discharges was also slightly greater than for one single discharge. This phenomenon can be explained by the following reasoning. Each discharge affects the treated VOCs by several simultaneous effects: direct electron-impact processes, thermal decomposition and reactions with radicals that induce decomposition processes in the post-discharge zone. The electron-impact processes, including charge exchange between the VOC molecule and positive ions from air (known for toluene), with consecutive dissociative recombination of the VOC ion with an electron, are by some authors considered dominant in non-thermal plasmas,<sup>[19, 20]</sup> despite the fact that they strongly depend on the electron density and temperature. In our discharge, (1) the electron and the positive ion densities are of the order

of  $10^{12} \text{ cm}^{-3}$ , i.e., four orders of magnitude lower than the density of the VOC molecules (at a concentration of 1 000–2 000 ppm); (2) the reduced field and therefore the electron temperature are low (40–65 Td); and (3) the electron-impact processes occur just in the plasma region in the discharge channels that take up a relatively small fraction of the whole reactor volume. We therefore cannot consider these processes to be significant in our case. The thermal VOC decomposition is probably more important due to relatively high temperature in the discharges ( $\sim 2\,000 \text{ K}$ ) but also occurs within a small volume in the discharge proximity. The radicals formed, on the other hand, may be active not only in the plasma region but also in more distant parts of the reactor volume. In addition, radical reactions have been found to be very important by many authors in VOC abatement, e.g., ref.,<sup>[22–25]</sup> especially the OH radical with toluene.<sup>[23–25]</sup> Our finding that the efficiency per discharge was the largest for two distant discharges supports the idea of the significance of radical reactions. Therefore, in order to take maximum advantage of the radical effect in the reactor, it seemed convenient to extend the post-discharge zone before the gas enters another discharge and undergoes another electron-impact and thermal treatment. Also bearing in mind the synergy effect of multiple discharges, this result suggests that with HPGD in the glass tube reactor, it is convenient to work with several (e.g. 5) low-energetic discharges distant from one another.

### Products

VOCs treated by the HPGD in the glass tube reactors were converted to some gaseous and some condensed products. The products were extensively analyzed by the FT-IR spectroscopy. Their character and concentrations depended on the discharge polarity, the presence of water vapor in the carrying air, the VOC type and initial concentration and especially on the energy density dissipated in the reactor.

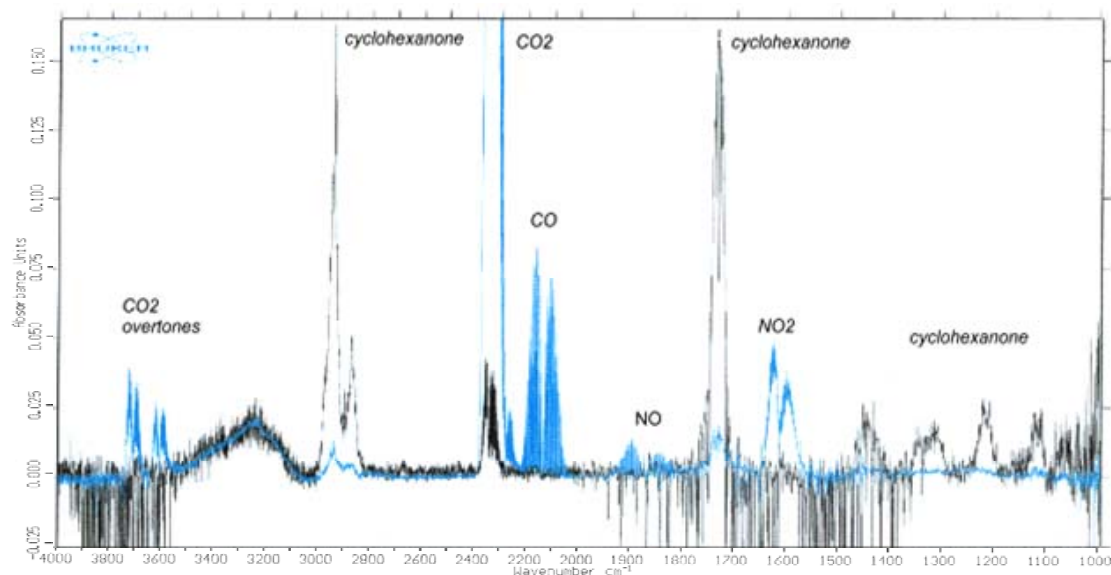


Figure 10. FT-IR spectrum of cyclohexanone (2 000 ppm) in humid air before (black) and after (blue) negative HPGD treatment in the 5-point reactor. Bands of the dominant gaseous products are identified.

The typical gaseous products were  $\text{CO}_2$  and  $\text{H}_2\text{O}$ , as well as some noxious gases such as  $\text{CO}$ ,  $\text{NO}_2$  and  $\text{NO}$ . In trace amounts,  $\text{HCHO}$ ,  $\text{HNO}_2$ ,  $\text{N}_2\text{O}$ , and alcohols (methanol, ethanol) were also detected and in humid air sometimes  $\text{HNO}_3$ . A representative FT-IR spectrum of 2 000 ppm cyclohexanone air mixture before and after the negative HPGD treatment in the 5-point glass tube reactor is shown in Figure 10.

The concentration of  $\text{CO}_2$  produced increased with the increasing  $w$ , as shown in Figure 11.  $\text{CO}_2$  concentrations of 600–6 000 ppm were formed from 2 000 ppm cyclohexanone, and 800–15 000 ppm from 2 000 ppm toluene.  $\text{CO}$  production first increased with  $w$ , then reached a maximum (at  $\sim 2\,500\text{ J.l}^{-1}$  for cyclohexanone and  $\sim 1\,500\text{ J.l}^{-1}$  for toluene), and finally decreased (see Figure 12). The  $\text{CO}$  concentrations produced were 600–1 600 ppm from cyclohexanone and 500–2 500 ppm from toluene, and slightly lower values in humid air. The  $\text{CO}/\text{CO}_2$  ratio decreased with  $w$  for both VOCs and both discharge polarities, being lower in the humid air (Figure 13). For cyclohexanone,  $\text{CO}/\text{CO}_2$  was from 1.5 to 0.1, and for toluene was from 1.2 to 0.05. With decreasing  $\text{CO}/\text{CO}_2$  ratio, the process moves closer to perfect combustion.

The carbon balance, i.e. the ratio between the carbon converted from VOCs to gaseous products and the total carbon treated in the process, is depicted in Figure 14. It typically varied from 40 % at low  $w$  to 80 % at high  $w$  for both VOCs, and in the negative polarity was sometimes as high as 100 %. These values correspond to about 20–60 % of the total treated carbon converted to non-gaseous products. The more thermal process leads to the greater formation of gaseous products, while at low  $w$ , mostly condensed products were formed. In air pollution control processes, condensed products generally tend to be avoided,

while non-toxic  $\text{CO}_2$  and  $\text{H}_2\text{O}$  are the most desired. Nonetheless, the production of toxic  $\text{CO}$  and  $\text{NO}_x$  usually accompanies  $\text{CO}_2$  and  $\text{H}_2\text{O}$ , and certain amounts of condensed products or aerosols are often formed as well. Furthermore, regarding  $\text{CO}_2$  as the main contributor to the Earth's enhanced greenhouse effect leads us to introduce a novel approach in the pollution control techniques: non-toxic condensed products may be more convenient than toxic or greenhouse gases. On an industrial scale, such an approach of course requires the problem of deposits and aerosols forming in the reactor to be addressed. For example, condensed products can be washed out and directed into existing systems for polluted water treatment.

The production of  $\text{NO}_x$  is typical for combustion-like processes occurring in air, including air plasmas with elevated gas temperatures. Graphs showing the concentrations of  $\text{NO}_2$  and  $\text{NO}$  produced as a function of the energy density for all four cases of cyclohexanone treatment in the 5-point glass tube reactor are shown in Figure 15 and 16. The  $\text{NO}_x$  concentrations produced were very similar with toluene treatment.  $\text{NO}_2$  and  $\text{NO}$  production increased with  $w$  in both polarities, and in dry as well as humid air. About 100–400 ppm of  $\text{NO}_2$  and 0–1 200 ppm of  $\text{NO}$  were produced. The lowest  $\text{NO}_x$  production occurred in the negative HPGD and humid air, which is probably due to the presence of water vapor and OH radicals.

Besides gaseous products, a white aerosol was often observed forming in the reactor. This aerosol was analyzed qualitatively by the FT-IR spectroscopy and all the functional groups of peroxy-acetyl-nitrates (PANs) were detected. It is suggested that this aerosol may be formed by a mechanism similar to the formation of photochemical smog in the atmosphere.

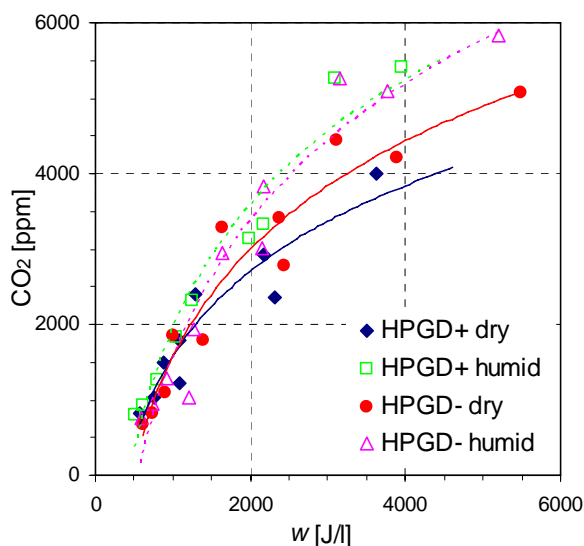


Figure 11. Formed  $\text{CO}_2$  concentration as a function of the energy density,  $w$ . Both polarities of HPGD in dry and humid air, 5-point glass tube reactor, cyclohexanone 2 000 ppm.

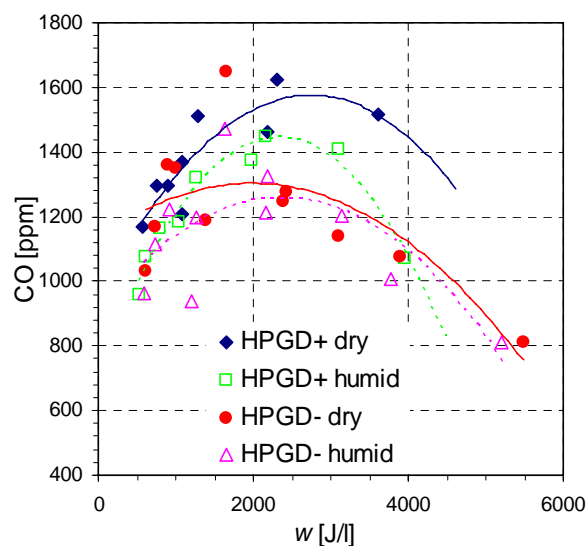


Figure 12. Formed  $\text{CO}$  concentration as a function of the energy density,  $w$ . Both polarities of HPGD in dry and humid air, 5-point glass tube reactor, cyclohexanone 2 000 ppm.

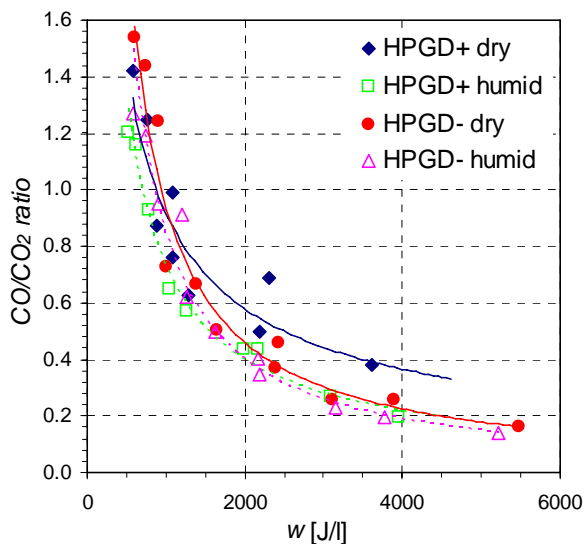


Figure 13. CO/CO<sub>2</sub> ratio as a function of the energy density,  $w$ . Both polarities of HPGD in dry and humid air, 5-point glass tube reactor, cyclohexanone 2 000 ppm.

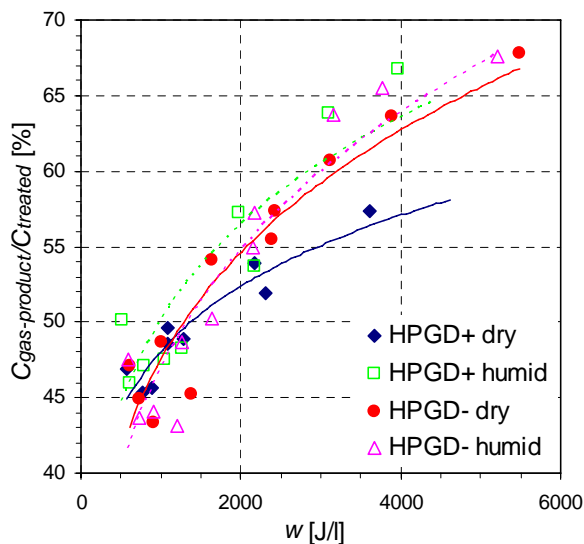


Figure 14. Treated carbon balance  $C_{\text{gas-product}}/C_{\text{treated}}$  as a function of the energy density,  $w$ . Both polarities of HPGD in dry and humid air, 5-point glass tube reactor, cyclohexanone 2 000 ppm.

Various liquid and solid deposits were also detected on the electrodes and reactor walls. They were extensively analyzed by the infrared absorption spectroscopy, and electron and optical microscopy. Condensates of different composition were formed at various parts of the reactor and the outlet, depending on the surface properties and the distance from the discharge.

The deposits condensed on the reactor walls were typically brown-yellow sticky viscose liquids soluble in acetone, ethanol and toluene, and almost insoluble in water.

Example FT-IR spectra are shown in Figure 17. The character of deposits formed on the electrodes depended on the electrode polarity and especially on the position with respect to the arriving discharge. Nearest to the discharge, these deposits formed hard brown-black polymer structures strongly attached to Cu surfaces and containing crystalline copper oxides (CuO and Cu<sub>2</sub>O). Their hard nature is probably due to the strongly elevated local electrode temperature. Farther from the discharge, the deposits gradually became amorphous, of a brown-gray color, and were partially soluble in organic solvents.

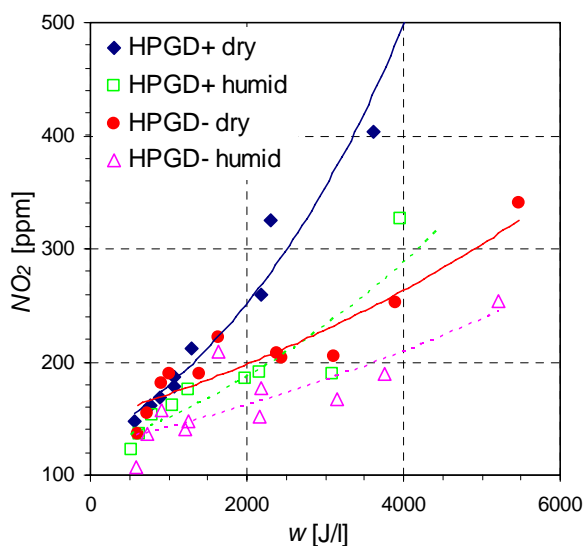


Figure 15. Formed NO<sub>2</sub> concentration as a function of the energy density,  $w$ . Both polarities of HPGD in dry and humid air, 5-point glass tube reactor, cyclohexanone 2 000 ppm.

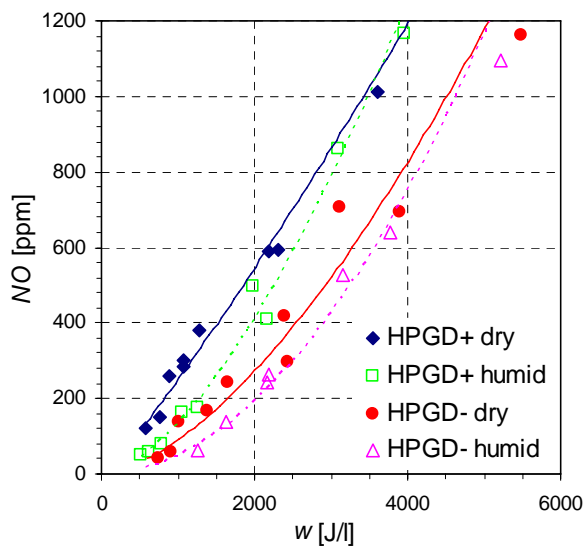


Figure 16. Formed NO concentration as a function of the energy density,  $w$ . Both polarities of HPGD in dry and humid air, 5-point glass tube reactor, cyclohexanone 2 000 ppm.



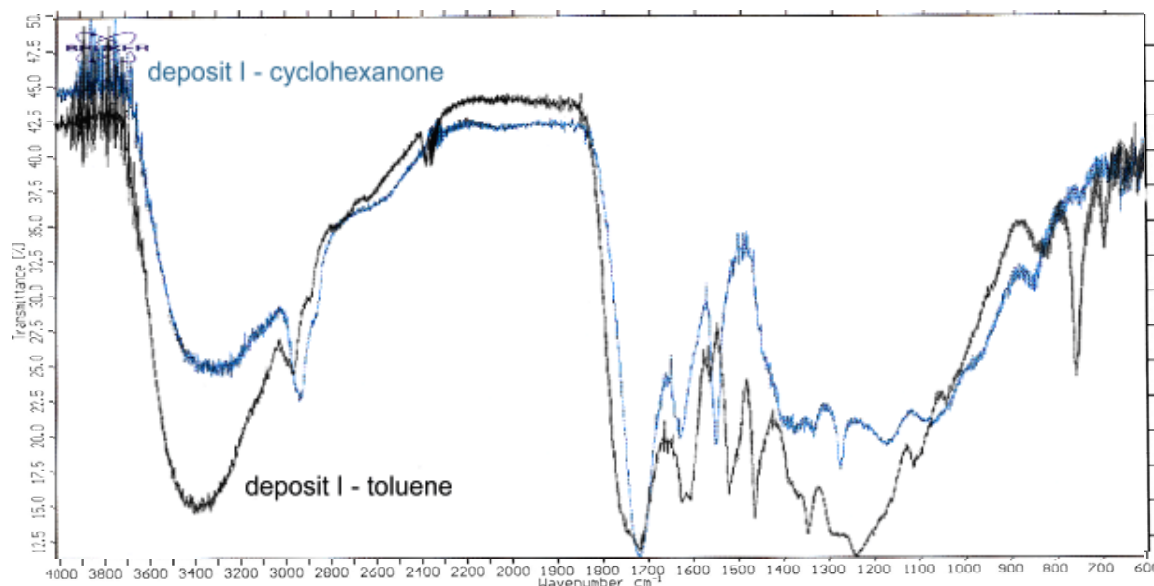


Figure 17. Typical IR spectrum of the liquid deposit condensed on the glass reactor walls formed from cyclohexanone and toluene.

Our analysis proved that the deposits contained C=O, OH, COOH, NH, NH<sub>2</sub>, -CO-NH- or -CO-N<, CH<sub>2</sub>, COO-, C-O-C and -NO<sub>2</sub> groups, and the deposits from toluene also contained aromatic rings. In most cases, the deposits were complex organic structures. Some of them, especially those forming on the electrodes farther from the discharge arrival zones, were, according to our analysis, likely to contain amino acids. It was observed that amino acids and similar structures were preferentially formed on the Cu electrode surfaces that seem to have certain catalytic effects on the process, in agreement with other studies.<sup>[26-27]</sup> The catalytic effects of copper electrodes were more pronounced in the Cu tube reactor. This reactor has considerably larger Cu electrode surfaces than the glass tube reactors, thereby enhancing the contact of the treated gas with the charged Cu surfaces. As a result, VOCs were destroyed at lower energy costs, and lower concentrations of gaseous products and aerosols and larger amounts of condensed products containing amino acids were obtained. Further investigations are needed to obtain a deeper insight into this matter.

## Conclusion

A stable atmospheric pressure DC discharge in ambient air has been presented. The discharge properties were those of a glow discharge, with a distinct cathode layer and positive column. This type of discharge provided a source of highly ionized nonequilibrium air plasma with electron number densities of the order of  $10^{12}$ - $10^{13}$  cm<sup>-3</sup>, and gas temperatures of 1 500-2 500 K. Relatively simple DC operation and convenient properties of the generated plasma make this discharge attractive for many applications, including air pollution control.

The DC discharge was tested for the abatement of selected VOCs (cyclohexanone and toluene) in glass and copper tube reactors. Removal efficiency increased

logarithmically with the energy density, reaching values as high as 95 %. The energy costs also increased with the energy density, reaching 200-1 000 eV/molecule. By comparing the effects of 1, 5, 10 and 2 distant discharges it was found that it was optimal to operate about 5 discharges that were distant from each other. This is most likely associated with the fact that the electron-impact and thermal VOC decomposition processes are coupled with radical-induced volume reactions. Putting the consecutive discharges far from each other extends the radical-dominated decomposition phase.

The VOCs tested were converted to some gaseous and some condensed products. Dominant gaseous products were CO<sub>2</sub>, CO, H<sub>2</sub>O, and NO<sub>x</sub>. Their concentrations depended on the initial VOC concentration, the presence of water vapors, reactor properties, and the energy density. The VOC removal process was partially similar to combustion characterized by a relatively low CO/CO<sub>2</sub> ratio. The negative discharge polarity and humid air resulted in the highest efficiencies, the lowest energy costs and the lowest concentrations of noxious outlet gases. A non-negligible part of the treated carbon from VOCs transformed to liquid and solid deposits, which formed on the reactor walls, and on the electrodes. The deposits were of complex organic structures, which depended on the place of their formation in the reactor. Cu electrode surfaces promoted the formation of amino acid-based products. They also seemed to have certain catalytic effects in the VOC abatement process.

*Acknowledgements:* The original work at University Paris XI was conducted during the Ph.D. studies of Z. Machala and was funded by a scholarship of the *French government*. The work performed at Comenius University was funded by VEGA 1/2013/05 and 1/0256/03 grants of the *Slovak grant agency*, and by *NATO* grant EAP.RIG 981194.

- [1] R.H. Stark and K.H. Schoenbach, *Appl. Phys. Lett.* **1999**, *74*, 3770.
- [2] P. Andre, Yu. Barinov, G. Faure, V. Kaplan, A. Lefort, S. Shkol'nik, D. Vacher, *J. Phys. D: Appl. Phys.* **2001**, *34*, 3456.
- [3] X. Lu, F. Leipold, M. Laroussi, *J. Phys. D: Appl. Phys.* **2003**, *36*, 2662.
- [4] Y. Yang, *IEEE Trans. Plasma Sci.* **2003**, *31*, 174.
- [5] Yu. Akishev, O. Goossens, T. Callebaut, C. Leys, A. Napartovich, N. Trushkin, *J. Phys. D: Appl. Phys.* **2001**, *34*, 2875.
- [6] O. Goossens, T. Callebaut, Yu. Akishev, A. Napartovich, N. Trushkin, C. Leys, *IEEE Trans. Plasma Sci.* **2002**, *30*, 176.
- [7] P. Mezei, T. Cserfalvi, M. Jánossy, *J. Phys. D: Appl. Phys.* **2001**, *34*, 1914.
- [8] L. Yu, C.O. Laux, D.M. Packan, and C.H. Kruger, *J. Appl. Phys.* **2002**, *91*, 2678.
- [9] X. Duten, D. Packan, L. Yu, C.O. Laux, C.H. Kruger, *IEEE Trans. Plasma Sci.* **2002**, *30*, 178.
- [10] Z. Machala, Ph.D. thesis, University Paris-Sud XI, France; Comenius University, Slovakia 2000.
- [11] Z. Machala, M. Morvová, E. Marode, I. Morva, *J. Phys. D: Appl. Phys.* **2000**, *33*, 3198.
- [12] Z. Machala, E. Marode, C. O. Laux, C. H. Kruger, *J. Advanced Oxid. Technol.* **2004**, *7* 133.
- [13] Z. Machala, E. Marode, C.O. Laux, C.H. Kruger, "DC discharges in atmospheric pressure air in the glow and glow-to-arc transition regimes" XV Int. Conf. Gas Discharges and Applications, Vol. 2, p. 1089-1092, Toulouse, France, September 2004
- [14] S. Pekárek, V. Kříha, M. Pospíšil, I. Viden, *J. Phys. D: Appl. Phys.* **2001**, *34*, 1.
- [15] R. Vertriest, R. Morent, J. Dewulf, C. Leys, H. Van Langenhove, *Plasma Sources Sci. Technol.* **2003**, *12*, 412.
- [16] K. Hensel, J. Pawlat, K. Takashima, A. Mizuno, "Possibilities of Formaldehyde Removal by Discharge Plasma", Proc. International Joint Power Generation Conference, Georgia (USA), paper IJPGC2003-40149, June 15-19, 2003.
- [17] N. Hayashi, H. Suganuma, M. Kamatani, S. Satoh, C. Yamabe, *Jpn. J. Appl. Phys.* **2001**, *40*, 6104.
- [18] A. Huczko, H. Lange, M. Sioda, Z. Ržanek-Boroch, M. Morvová, *Czech. J. Phys.* **2000**, *50*, 615.
- [19] H. Kohno, A.A. Berezin, J.-S. Chang, M. Tamura, T. Yamamoto, A. Shibuya, S. Honda, *IEEE Trans. Ind. Appl.* **1998**, *34*, 953.
- [20] K. Urashima and J.-S. Chang, *IEEE Trans. Dielectrics Elec. Insul.* **2000**, *7*, 602.
- [21] Yu.P. Raizer, "Gas Discharge Physics", Springer, New York 1991, pp. 182 and 11.
- [22] M.B. Chang and C.C. Chang, *AIChE J.* **1997**, *43*, 1325.
- [23] R. Rudolph, K.P. Francke, H. Miessner, *Plasmas and Polymers* **2003**; *8*, 153.
- [24] R. Rudolph, K.P. Francke, H. Miessner, *Plasma Chem. Plasma Process.* **2002**, *22*, 401.
- [25] Z.L. Wu, X. Gao, Z.Y. Luo, M.J. Ni, K.F. Cen, *J. Env. Sci.-China* **2004**, *16*, 543.
- [26] R. Gasparik, C. Yamabe, S. Ihara and S. Satoh, *Jpn. J. Appl. Phys.* **1998**, *37*, 5786.
- [27] F. Hanic, M. Morvová, I. Morva, *J. Thermal Analysis Calorimetry* **2000**, *60*, 1111.